Low-frequency currents induced in adjacent spherical cells

Dionisios Margetis and Nikos Savva
Department of Mathematics, Massachusetts Institute of Technology, Cambridge, Massachusetts 02139

(Received 4 September 2005; accepted 3 March 2006; published online 21 April 2006)

The currents induced inside cells by external electric fields in the frequency range 50–60 Hz are studied analytically by accounting for thin cell membranes with transverse conductivity that is small compared to the conductivity of the saline fluid. A general perturbation scheme is formulated and applied to two adjacent spherical cells of equal radii by using a reflection principle and solving a nonlinear difference equation. The presence of the second cell is found to cause a no more than 10% increase to the current induced in an isolated spherical cell. © *2006 American Institute of Physics.* [DOI: 10.1063/1.2190333]

I. INTRODUCTION

Concerns about the possible health effects of electromagnetic fields generated by power lines have stimulated theoretical studies of the currents induced in the human body when this is exposed to external, extremely-low-frequency fields, in the frequency range 50–60 Hz.[1–11] Over a decade ago Adair[2] asserted that the current induced inside an isolated cell is negligible, because the resistive cell membrane appears to shield the cell interior from incident low-frequency fields.

More recently, King and Wu[4] pointed out that Adair's conclusion, although correct for spherical cells, may not be valid for elongated, cylindrical cells. In the latter case the induced current depends on the length of the cell and the polarization of the incident electric field, so that shielding effects can be significantly reduced as the cell length increases or the incident field becomes parallel to the cell axis. For a typical spherical cell with radius 1 μm, membrane thickness $\delta \approx 5$ nm, membrane conductivity $\sigma_m \approx 10^{-6}$ S/m, and protoplasm (saline-fluid) conductivity $\sigma_0 \approx 0.5$S/m, King and Wu[4] calculated the electric field to be reduced by a factor 10^{-4} inside the cell. By contrast, the electric field inside the elongated, myelinated cell was calculated[4] to be almost equal to the incident field if the length of the cell roughly exceeds 5 mm and the external field is along the cell axis.

The purpose of the present study is to extend previous works[2,4] to more realistic cases where the current induced inside a cell is affected by the presence of neighboring cells. As a starting point, we treat the geometry with two spherical cells by an analytical technique which is directly applicable, although increasingly cumbersome, to many-cell geometries. Our formulation considers disconnected cells and therefore differs from that of Ref. 5 where cells are connected through suitable gap junctions.

The main assumptions underlying our analysis are that the cell membrane thickness is small compared to (i) the cell radius of curvature, and (ii) the length over which the cell curvature varies. So, elongated cells with sharp ends may not be included in the analysis. In addition, the cell curvature is assumed to be a sufficiently smooth and slowly varying function of the surface coordinates. Following Ref. 4 we also assume that the cell membrane is homogeneous and isotropic, with a scalar conductivity σ_m in the range 10^{-5}–10^{-6} S/m. This assumption may pose a limitation on our model, especially because membranes of actual cells have ion channels[12] and thus act as anisotropic media. To avoid complications due to anisotropies and yet preserve the essential physical features of thin membranes we replace the membrane by an "effective" boundary condition that accounts for its thickness and conductivity in the direction transverse to the cell

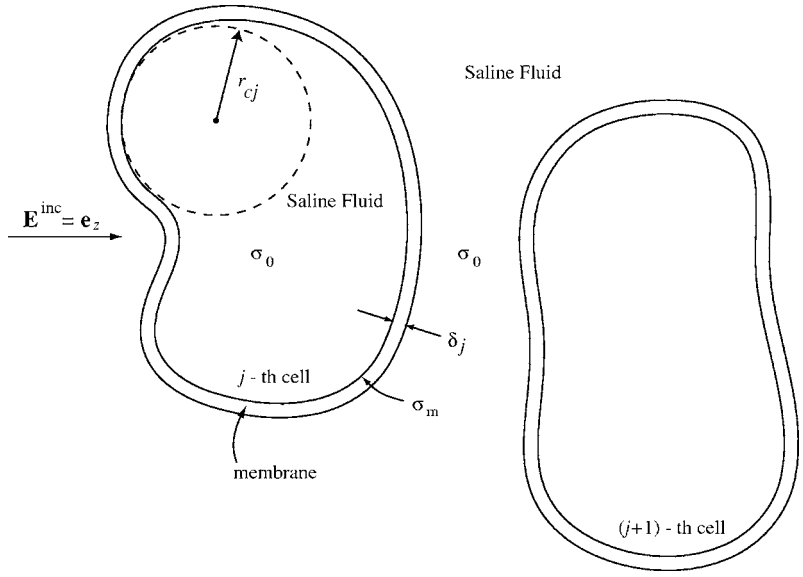

FIG. 1. Schematic of the geometry of arbitrarily shaped cells. The jth cell has radius of curvature r_{cj} and membrane thickness δ_j. The conductivities of the saline fluid and cell membrane are σ_0 and σ_m, respectively. The incident electric field is polarized along the **z** axis.

surface;[4] cf. Eq. (9) below. Similarly, the cell interior is considered as homogeneous and isotropic with conductivity σ_0, typically in the range $0.5-0.8$ S/m, which is taken to be equal to the conductivity of the surrounding saline fluid.

One can argue that the reduction of the electric field in the interior of a cell of reasonably arbitrary shape can be estimated by dimensional analysis. More precisely, the fraction of the penetrating field is expected to be proportional to the *small* factor $\tilde{\epsilon}=(\bar{r}_c/\delta)(\sigma_m/\sigma_0)$, where $\bar{r}_c$ is the cell mean radius of curvature, typically in the range $1-10$ μm, and δ is the membrane thickness, $\delta=2-5$ nm; cf. Fig. 1. This observation motivates the perturbation analysis of this paper because it indicates the dependence of the induced current on the small dimensionless parameter $\tilde{\epsilon}$. A similar technique is described in Ref. 13 for the cell response to a delta-function excitation. The application of perturbation theory, as described below, transcends dimensional analysis because it provides (i) a general mathematical framework to treat systematically problems of low-frequency scattering by cells; and (ii) a closed-form formula for the geometry-dependent prefactor for the field reduction inside a cell for the practically appealing case with two spherical cells of equal radii.

The paper is organized as follows. In Sec. II we describe the general formulation based on perturbation theory to determine currents induced inside cells exposed to uniform electric fields. In Sec. III we apply this formulation to the case with two neighboring spherical cells and derive simple, closed-form formulas for the electric field in the interior of each of the cells. In Sec. IV we discuss other cell geometries where the present framework may serve as a basis of detailed studies. The $e^{-i\omega t}$ time dependence is suppressed throughout the analysis.

II. PERTURBATION THEORY

A. General formulation

We consider a uniform electric field $\mathbf{E}^{\text{inc}}$ parallel to the **z** axis, $\mathbf{E}^{\text{inc}}=E_0\mathbf{e}_z$, and incident upon N cells of reasonably arbitrary shape, where $\mathbf{e}_z$ is the **z**-directed unit vector of the Cartesian coordinate system, and we take $E_0=1$ without loss of generality; cf. Fig. 1. The cells are immersed in saline fluid, an isotropic and homogeneous medium with conductivity σ_0. The interior $\mathcal{R}_j$ of the jth cell[14] is also assumed to be isotropic and homogeneous with a conductivity σ_0, equal to that of the ambient medium. The membrane is sufficiently thin and in principle anisotropic; we take the

membrane conductivity in the direction normal to the boundary to be σ_m, which is small compared to σ_0, $\sigma_m \ll \sigma_0$. At sufficiently low frequencies the effective dielectric constant, ϵ_{eff}, in each medium is dominated by the corresponding conductivity σ,

$$\epsilon_{\text{eff}} \sim \frac{i\sigma}{\omega}, \tag{1}$$

where ω is the radial frequency of the incident field.

The electric field inside each cell depends on the *relative* effective dielectric constant of the membrane because the requisite boundary conditions for the field on the cell surfaces, through which the conductivities enter, are homogeneous; see Appendix A where the problem of a single spherical cell is revisited. Therefore, for later notational convenience we introduce the dimensionless parameter ϵ by

$$\epsilon = \frac{\sigma_m}{\sigma_0}, \tag{2}$$

where ϵ is a small positive number, $0 < \epsilon \ll 1$.

The local radius of curvature, r_{cj}, of the jth cell is assumed to be a positive, sufficiently smooth function of the surface coordinates, and large compared to the membrane thickness δ_j,[15]

$$\tilde{r} = \frac{r_{cj}}{\delta_j} \gg 1. \tag{3}$$

Effective boundary conditions at the boundaries of cells with thin membranes involve the parameter $\tilde{r}\epsilon$.[4] In many cell configurations of interest this parameter is small,

$$\tilde{r}\epsilon \ll 1. \tag{4}$$

Condition (4) is enforced throughout the paper, and enables the application of regular perturbation theory as described below; see also Appendix A where, by virtue of (4), a simplified formula is derived for the current in the interior of an isolated spherical cell.

When the frequency of the incident electromagnetic field is sufficiently low, for instance in the range 50–60 Hz, a mathematically convenient quantity to use is the scalar potential, $\Phi(\mathbf{r})$, which satisfies to a good approximation the Laplace equation,

$$\nabla^2 \Phi(\mathbf{r}) = 0. \tag{5}$$

The electric field $\mathbf{E}(\mathbf{r})$ is approximately decoupled from the magnetic field, and is described by

$$\mathbf{E} = -\nabla\Phi. \tag{6}$$

For the incident field $\mathbf{E}^{\text{inc}} = \mathbf{e}_z$ the condition for $\Phi(\mathbf{r})$ at infinity reads

$$\Phi(\mathbf{r}) \sim -z, \quad r = |\mathbf{r}| \to \infty. \tag{7}$$

Despite the simple form of (5) and (6), mathematical complications may arise because of the special boundary conditions at the membrane separating the cell interior from the saline fluid. Following Ref. 4 we replace the membrane by an effective boundary condition that stems from treating the membrane thickness, δ_j, as properly small compared to the membrane radius of curvature. Next, we rederive briefly and interpret the related result of Ref. 4 by relaxing mathematical elaboration. By integration of (6) across the membrane, the restriction Φ^+ of Φ on the cell boundary from outside the cell and the corresponding restriction Φ^- from inside the cell should satisfy $\Phi^+ - \Phi^- = -E_{m,\perp}\delta_j$; $E_{m,\perp}$ is an appropriate value of the electric field normal to the boundary *inside* the membrane and $\Phi^{\pm}$ are boundary values of Φ *outside* the membrane. For suitably thin membrane, $E_{m,\perp}$ satisfies $\sigma_m E_{m,\perp} = \sigma_0 E_\perp^+ = \sigma_0 E_\perp^-$ by Gauss's law in the absence of surface charge,

where $E_{\perp}^{\pm}$ denote the boundary values of the transverse electric field outside the membrane. The relations of this paragraph yield

$$\frac{\partial \Phi^{+}}{\partial \eta} = \frac{\partial \Phi^{-}}{\partial \eta} \equiv \left. \frac{\partial \Phi}{\partial \eta} \right|_{\partial \mathcal{R}_j}, \tag{8}$$

$$\left. \frac{\partial \Phi}{\partial \eta} \right|_{\partial \mathcal{R}_j} = \frac{1}{\xi_j} [\Phi^{+}(\mathbf{r}) - \Phi^{-}(\mathbf{r})], \tag{9}$$

where $\partial \mathcal{R}_j$ is the boundary of region $\mathcal{R}_j$, $\partial \Phi / \partial \eta = \mathbf{e}_\eta \cdot \nabla \Phi$ and $\mathbf{e}_\eta$ is the unit vector normal to the boundary $\partial \mathcal{R}_j$ pointing outward; $\Phi^{+}(\mathbf{r})$ and $\partial \Phi^{+} / \partial \eta$ are the values of Φ and $\partial \Phi / \partial \eta$ as $\mathbf{r}$ approaches $\partial \mathcal{R}_j$ from outside the cell ($\mathbf{r} \to \partial \mathcal{R}_j^{+}$), and $\Phi^{-}(\mathbf{r})$ and $\partial \Phi^{-} / \partial \eta$ are the corresponding values as $\mathbf{r}$ approaches $\partial \mathcal{R}_j$ from inside the cell ($\mathbf{r} \to \partial \mathcal{R}_j^{-}$). The parameter ξ_j has dimensions of length and is defined by

$$\xi_j = \frac{\delta_j}{\epsilon}. \tag{10}$$

Condition (4) ensures that the ξ_j entering boundary condition (9) is large compared to the radius of cell curvature, r_{cj},

$$r_{cj} \ll \xi_j. \tag{11}$$

Next, we describe a perturbation scheme for calculating Φ. The starting point is the expansion[16]

$$\Phi = \Phi_0 + \Phi_1 + \cdots + \Phi_n + \cdots, \quad n = 0, 1, \ldots, \tag{12}$$

where the subscript, n, denotes the perturbation order[17] and the ratio of two successive terms is assumed to be[18]

$$\frac{\Phi_n}{\Phi_{n-1}} = O\left(\frac{r_{c1}}{\xi_1}, \ldots, \frac{r_{cN}}{\xi_N} \right). \tag{13}$$

Each term Φ_n in expansion (12) is determined iteratively as described below.

1. Zeroth-order approximation, n=0

In the zeroth-order approximation the right-hand side of (9) is set equal to zero. With $\Phi(\mathbf{r}) \sim \Phi_0(\mathbf{r})$, Φ_0 satisfies Laplace's equation and the Neumann boundary condition on the cell boundaries, $\partial \mathcal{R}_j$. The boundary-value problem for the cell exterior thus reads

$$\nabla^2 \Phi_0(\mathbf{r}) = 0, \quad \mathbf{r} \in \Omega, \qquad \left. \frac{\partial \Phi_0}{\partial \eta} \right|_{\partial \mathcal{R}_j^{+}} = 0, \quad j = 1, 2, \ldots, N, \tag{14}$$

along with condition (7), where $\Omega = \mathbb{R}^3 - \cup_j \mathcal{R}_j - \cup_j \partial \mathcal{R}_j$ is the exterior of all cells ($\mathcal{R}_j$) with exclusion of every $\partial \mathcal{R}_j$; $\mathbb{R}^3$ is the Euclidean space. This problem admits a unique solution for $\Phi_0(\mathbf{r})$.[19] The corresponding problem for the cell interior $\mathcal{R}_j$ has solution

$$\Phi_0(\mathbf{r}) = \varphi_{0j}, \quad \mathbf{r} \in \mathcal{R}_j, \tag{15}$$

where φ_{0j} ($j = 1, 2, \ldots, N$) are constants to be determined below. Each of these constants enters the boundary conditions for $\Phi_1(\mathbf{r})$ (in the first-order approximation) and is evaluated as an appropriate surface integral of $\Phi_0(\mathbf{r})$; cf. (19) below.

2. First-order approximation, $n=1$

In this approximation the right-hand side of (9) is replaced by $(\Phi_0^+ - \Phi_0^-)/\xi_j$, and $\Phi(\mathbf{r}) \sim \Phi_0(\mathbf{r}) + \Phi_1(\mathbf{r})$ where $\Phi_0(\mathbf{r})$ is known from (14) above. The boundary-value problem for the cell interior is described by

$$\nabla^2 \Phi_1(\mathbf{r}) = 0, \quad \mathbf{r} \in \mathcal{R}_j, \qquad \left.\frac{\partial \Phi_1}{\partial \eta}\right|_{\mathbf{r} \in \partial \mathcal{R}_j^-} = \frac{1}{\xi_j}(\Phi_0^+ - \varphi_{0j}), \tag{16}$$

along with the condition that $\Phi_1(\mathbf{r})$ be finite in $\mathcal{R}_j$. The Laplace equation with the same boundary conditions on $\partial \mathcal{R}_j$ also apply to the exterior problem. The requisite condition for Φ_1 at infinity becomes

$$\Phi_1(\mathbf{r}) \to 0, \quad r \to \infty. \tag{17}$$

Because the constant φ_{0j} enters the Neumann condition (16), its value must be consistent with the Laplace equation.[19] By integrating $\nabla^2 \Phi_1 = 0$ over $\mathcal{R}_j$ we obtain

$$\oint_{\partial \mathcal{R}_j^-} d\mathbf{r}\, \frac{\partial \Phi_1}{\partial \eta} = 0. \tag{18}$$

By virtue of condition (16),

$$\varphi_{0j} = \frac{1}{\|\partial \mathcal{R}_j\|} \oint_{\partial \mathcal{R}_j} d\mathbf{r}\, \Phi_0^+(\mathbf{r}), \tag{19}$$

where $\|\partial \mathcal{R}_j\|$ denotes the area of the closed surface $\partial \mathcal{R}_j$.

3. nth-order approximation, $n=1,2,\ldots$

It is reasonably straightforward to generalize the first-order approximation in order to carry out the calculations to the next orders in r_{cj}/ξ_j. With $\Phi(\mathbf{r}) \sim \Sigma_{i=0}^n \Phi_i(\mathbf{r})$ and $n \geqslant 1$ the boundary-value problem for $\Phi_n(\mathbf{r})$ follows from the preceding discussions of the zeroth- and first-order approximations via the replacements $0 \to n-1$ and $1 \to n$ in the subscripts for Φ. In the cell interior, Φ_n satisfies the boundary-value problem

$$\nabla^2 \Phi_n(\mathbf{r}) = 0, \quad \mathbf{r} \in \mathcal{R}_j, \qquad \left.\frac{\partial \Phi_n}{\partial \eta}\right|_{\partial \mathcal{R}_j^-} = \frac{1}{\xi_j}(\Phi_{n-1}^+ - \Phi_{n-1}^-), \tag{20}$$

where $\Phi_n(\mathbf{r})$ must be bounded everywhere for $n \geqslant 1$. The same differential equation and conditions on $\partial \mathcal{R}_j$ hold for the exterior problem. The condition at infinity reads

$$\Phi_n(\mathbf{r}) \to 0, \quad r \to \infty, \quad n \geqslant 1. \tag{21}$$

In the following we restrict the analysis to the zeroth- and first-order approximations for Φ.

B. Example: Single spherical cell

Next, for comparison and validation purposes we apply the general perturbation scheme of Sec. II A to a single spherical cell with radius a exposed to a uniform field $E^{\text{inc}} = \mathbf{e}_z$. This prototypical case was studied in Refs. 2 and 4. Here, we derive the same result as in Ref. 4 for the electric field inside the cell within the framework of our Sec. II A. For the sake of completeness, the derivation of Ref. 4 for a single cell is revisited in our Appendix A, via the full set of boundary conditions by which the cell membrane is taken to have a finite thickness.

1. Zeroth-order approximation

The potential Φ_0 of the exterior problem satisfies

$$\nabla^2\Phi_0(\mathbf{r}) = 0, \quad r > a, \tag{22}$$

and

$$\frac{\partial\Phi_0}{\partial r} = 0 \quad \text{at } r = a, \quad \Phi_0(r,\theta) \sim -z, \quad r \to \infty. \tag{23}$$

The solution to (22) and (23) is obtained via a reflection principle in Appendix B. The result is

$$\Phi_0(r,\theta) = -\left(r + \frac{a^3}{2r^2}\right)\cos\theta, \quad r > a. \tag{24}$$

In particular, for $r \to a^+$,

$$\Phi_0(a^+,\theta) = \Phi_0^+ = -\frac{3a}{2}\cos\theta. \tag{25}$$

It follows from (15) and (19) that the potential Φ_0 vanishes for $r < a$,

$$\Phi_0(r < a, \theta) \equiv \varphi_0 = 0. \tag{26}$$

2. First-order approximation

In the next order the interior problem is described by

$$\nabla^2\Phi_1(\mathbf{r}) = 0, \quad r < a, \tag{27}$$

$$\frac{\partial\Phi_1}{\partial r} = \frac{1}{\xi}\Phi_0^+ = -\frac{1}{\xi}\frac{3a}{2}\cos\theta \quad \text{at } r = a, \quad \Phi_1(0,\theta)\text{: finite}. \tag{28}$$

Recall that the parameter ξ is defined by (10). Because of rotational symmetry, we apply separation of variables and write $\Phi_1(r,\theta) = g(r)\cos\theta$ where, by (27) and (28), $g(r)$ satisfies

$$r^2\frac{d^2g}{dr^2} + 2r\frac{dg}{dr} - 2g = 0 \quad \text{for } r < a, \quad g(0)\text{: finite}, \quad g(a) = -\frac{3a}{2\xi}, \tag{29}$$

with solution $g(r) = -(3a/2\xi)r$. Hence,

$$\Phi_1(r,\theta) = -\frac{3a}{2\xi}r\cos\theta, \quad r < a, \tag{30}$$

in agreement with (A9) of Appendix A. The electric field $\mathbf{E}$ inside the sphere follows by $\mathbf{E} = -\nabla\Phi$,

$$\mathbf{E}(r,\theta) = \frac{3a}{2\xi}\mathbf{e}_z, \quad r < a. \tag{31}$$

This formula shows that the incident field is reduced by the factor $3a/2\xi$ inside the cell.[2,4]

III. PAIR OF SPHERICAL CELLS

In this section we apply the perturbation scheme introduced in Sec. II to two spherical cells, denoted A and B, with equal radii; cf. Fig. 2 for the geometry of the problem. The radius of each sphere is a and the distance between their centers, O_1 and O_2, is $2d$. The z axis passes through $O_1(0,0,-d)$ and $O_2(0,0,d)$. The extension of our treatment to two spherical cells with different radii, or to three or more spherical cells, is straightforward yet increasingly cumbersome and lies beyond the scope of this paper.

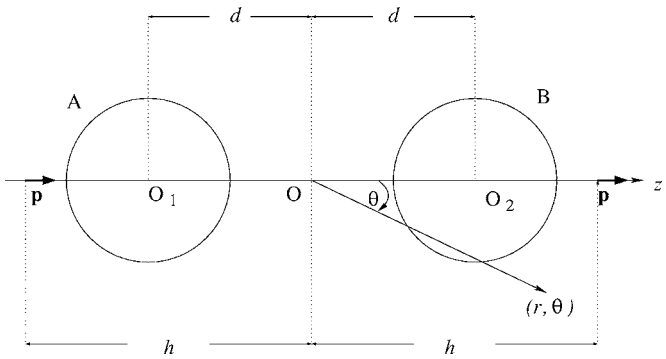

FIG. 2. The geometry of two spherical cells with equal radii, a. The incident, uniform electric field is polarized along the **z** axis. Two dipoles of moment $\mathbf{p}=\mathbf{e}_z$ are placed symmetrically with respect to the origin O in order to produce the incident field in the limit $h\to\infty$.

A. Zeroth-order approximation

The zeroth-order potential Φ_0 satisfies the Neumann boundary condition

$$\frac{\partial\Phi_0}{\partial\eta}=0, \quad \mathbf{r}\in\partial\mathcal{R}_A\cup\partial\mathcal{R}_B, \tag{32}$$

where $\partial\mathcal{R}_A$ and $\partial\mathcal{R}_B$ are the boundaries of spheres $\mathcal{R}_A$ and $\mathcal{R}_B$. In addition, $\Phi_0\sim -r\cos\theta$ as $r\to\infty$. We apply the reflection principle of Appendix B to the boundary-value problem for Φ_0 in the exterior of the cells by replacing the incident electric field by two electric dipoles (sources) of unit moment, $\mathbf{p}=\mathbf{e}_z$, located symmetrically with respect to O, at positions $(0,0,-h)$ and $(0,0,h)$; cf Fig. 2. The uniform incident field of unit amplitude, $\mathbf{E}^{\text{inc}}=\mathbf{e}_z$, is reproduced by taking the limit $h\to\infty$ after multiplying each (unit) dipole moment by πh^3; cf. (B10) of Appendix B. For finite h, the source dipoles generate an infinite number of image dipoles, all lying in the z axis, that are needed to sustain condition (32) on each spherical surface.

Next, we describe the location of image dipoles and their corresponding moments needed to satisfy the Neumann condition on the surface of each sphere, applying the results of Appendix B. Because each time an image dipole is placed inside a sphere the Neumann condition on the other sphere no longer holds, the procedure of placing image dipoles must be repeated *ad infinitum* leading to appropriate sequences of image dipoles inside each sphere. The source dipole at $(0,0,-h)$ induces image dipoles inside sphere A at positions $(0,0,-d-b),(0,0,-d+a_2),\ldots,(0,0,-d+a_{2j})$, and at $(0,0,-d+b_2),\ldots,(0,0,-d+b_{2j})$, and inside sphere B at positions $(0,0,d-a_1),\ldots,(0,0,d-a_{2j-1})$ and at $(0,0,b_1),\ldots,(0,0,d-b_{2j-1})$, where j here is a positive integer and $j\to\infty$. By symmetry, the dipole at $(0,0,h)$ induces images of equal corresponding moments inside sphere B at $(0,0,d+b)$, $(0,0,d-a_2),\ldots,(0,0,d-a_{2j})$ and at $(0,0,d-b_2),\ldots,(0,0,d-b_{2j})$, and inside sphere A at $(0,0,-d+a_1),\ldots,(0,0,-d+a_{2j+1})$ and at $(0,0,-d+b_1),\ldots,(0,0,-d+b_{2j+1})$. According to (B5) of Appendix B, the distance b is defined by

$$b=\frac{a^2}{h-d}. \tag{33}$$

The distances a_m and b_m, where $a_0=d-h$ and $b_0=-b$, separately satisfy the recursion relation

$$\alpha_m=\frac{a^2}{2d-\alpha_{m-1}}, \quad m=1,2,\ldots, \tag{34}$$

where $\alpha_0=a_0$ or $\alpha_0=b_0=-b$. It follows from (B7) of Appendix B that the moments of the image dipoles located at distances a_m from O_1 or O_2 are

$$p_m = (-1)^m \left(\frac{\prod_{i=1}^{m} a_i}{a^m} \right)^3, \quad m = 1,2,\ldots . \tag{35}$$

The dipole moments corresponding to distances b_m from O_1 or O_2 are

$$q_m = (-1)^{m+1} \left(\frac{b\prod_{i=1}^{m} b_i}{a^{m+1}} \right)^3, \quad m = 1,2,\ldots ; \quad q_0 = -(b/a)^3. \tag{36}$$

The difference equation (34) is solved in Appendix C to yield

$$\alpha_m = a \frac{\sinh[m\kappa - \zeta(\alpha_0)]}{\sinh[(m+1)\kappa - \zeta(\alpha_0)]}, \tag{37}$$

where

$$\kappa = \ln \lambda, \quad \lambda = \frac{d + \sqrt{d^2 - a^2}}{a}, \tag{38}$$

$$\zeta(\alpha) = \frac{1}{2} \ln \left[\frac{1 - \lambda a^{-1} \alpha}{1 - (\lambda a)^{-1} \alpha} \right]. \tag{39}$$

It follows from Eqs. (35) and (36) that the strengths of the image dipoles are given explicitly by

$$p_m = (-1)^m \left\{ \frac{\sinh[\kappa - \zeta(a_0)]}{\sinh[(m+1)\kappa - \zeta(a_0)]} \right\}^3, \quad m = 1,2,\ldots , \tag{40}$$

$$q_m = (-1)^{m+1} \left\{ \frac{\sinh \zeta(b_0)}{\sinh[(m+1)\kappa - \zeta(b_0)]} \right\}^3, \quad m = 0,1,2,\ldots . \tag{41}$$

Thus, the zeroth-order potential in the exterior of the cells is furnished by[20]

$$\begin{aligned} 4\pi\Phi^{\mathrm{d}}(\mathbf{r};h) = {} & \frac{\mathbf{e}_z \cdot (h\mathbf{e}_z + \mathbf{r})}{|h\mathbf{e}_z + \mathbf{r}|^3} + \frac{\mathbf{e}_z \cdot (-h\mathbf{e}_z + \mathbf{r})}{|-h\mathbf{e}_z + \mathbf{r}|^3} - \frac{b^3}{a^3} \frac{\mathbf{e}_z \cdot [(d+b)\mathbf{e}_z + \mathbf{r}]}{|(d+b)\mathbf{e}_z + \mathbf{r}|^3} - \frac{b^3}{a^3} \frac{\mathbf{e}_z \cdot [-(d+b)\mathbf{e}_z + \mathbf{r}]}{|-(d+b)\mathbf{e}_z + \mathbf{r}|^3} \\ & + \sum_{m=1}^{\infty} p_m \left[\frac{(d-a_m) + \mathbf{e}_z \cdot \mathbf{r}}{|(d-a_m)\mathbf{e}_z + \mathbf{r}|^3} + \frac{-(d-a_m) + \mathbf{e}_z \cdot \mathbf{r}}{|-(d-a_m)\mathbf{e}_z + \mathbf{r}|^3} \right] + \sum_{m=1}^{\infty} q_m \left[\frac{(d-b_m) + \mathbf{e}_z \cdot \mathbf{r}}{|(d-b_m)\mathbf{e}_z + \mathbf{r}|^3} \right. \\ & \left. + \frac{-(d-b_m) + \mathbf{e}_z \cdot \mathbf{r}}{|-(d-b_m)\mathbf{e}_z + \mathbf{r}|^3} \right] = \sum_{m=0}^{\infty} (-1)^m \left\{ \frac{\sinh[\kappa - \zeta(a_0)]}{\sinh[(m+1)\kappa - \zeta(a_0)]} \right\}^3 \left[\frac{(d-a_m) + \mathbf{e}_z \cdot \mathbf{r}}{|(d-a_m)\mathbf{e}_z + \mathbf{r}|^3} \right. \\ & \left. + \frac{-(d-a_m) + \mathbf{e}_z \cdot \mathbf{r}}{|-(d-a_m)\mathbf{e}_z + \mathbf{r}|^3} \right] + \sum_{m=0}^{\infty} (-1)^{m+1} \left\{ \frac{\sinh \zeta(b_0)}{\sinh[(m+1)\kappa - \zeta(b_0)]} \right\}^3 \left[\frac{(d-b_m) + \mathbf{e}_z \cdot \mathbf{r}}{|(d-b_m)\mathbf{e}_z + \mathbf{r}|^3} \right. \\ & \left. + \frac{-(d-b_m) + \mathbf{e}_z \cdot \mathbf{r}}{|-(d-b_m)\mathbf{e}_z + \mathbf{r}|^3} \right], \end{aligned} \tag{42}$$

where $a_0 = d - h$ and $b_0 = -b$. Recall that b is defined by (33).

In the limit $h \to \infty$ we obtain $a_0 \to -\infty$ and $b_0 \to 0$, and in view of (37) and (39) we find

$$\zeta(a_0) \sim \kappa - \frac{a}{h}\sinh\kappa, \quad \zeta(b_0) \sim \frac{a}{h}\sinh\kappa, \tag{43}$$

and

$$a_{m+1} \sim a\,\frac{\sinh(m\kappa)}{\sinh[(m+1)\kappa]} \equiv \chi_m, \quad b_m \sim \chi_m. \tag{44}$$

After some rearrangement of terms in (42), the potential for $h\to\infty$ reduces to

$$4\pi\Phi^{\mathrm{d}}(\mathbf{r};h) \sim -\frac{4}{h^3}z - 2\frac{a^3}{h^3}(\sinh\kappa)^3\sum_{m=0}^{\infty}\frac{(-1)^m}{[\sinh(m+1)\kappa]^3}\left\{\frac{d-\chi_m+z}{[(d-\chi_m)^2+r^2+2(d-\chi_m)z]^{3/2}}\right.$$
$$\left.+\frac{-(d-\chi_m)+z}{[(d-\chi_m)^2+r^2-2(d-\chi_m)z]^{3/2}}\right\}. \tag{45}$$

The zeroth-order potential $\Phi_0(\mathbf{r})$ is obtained via multiplying Φ^{d} above by πh^3 so that the potential at infinity becomes $-z$:

$$\Phi_0(\mathbf{r}) = \lim_{h\to\infty}(\pi h^3\Phi^{\mathrm{d}}) = -z - \frac{a^3}{2}(\sinh\kappa)^3\sum_{m=0}^{\infty}\frac{(-1)^m}{[\sinh(m+1)\kappa]^3}\left\{\frac{d-\chi_m+z}{[(d-\chi_m)^2+r^2+2(d-\chi_m)z]^{3/2}}\right.$$
$$\left.+\frac{-(d-\chi_m)+z}{[(d-\chi_m)^2+r^2-2(d-\chi_m)z]^{3/2}}\right\}. \tag{46}$$

For nontouching spheres ($d>a$) the terms of the preceding series approach zero exponentially fast as $m\to\infty$.

Equation (46) is simplified considerably when the spheres touch ($d\to a$). With

$$\kappa \sim \sqrt{2}\left(1-\frac{a}{d}\right)^{1/2} \to 0 \quad \text{as } d\to a, \tag{47}$$

(44) furnishes

$$\chi_m = a\,\frac{m}{m+1}. \tag{48}$$

Accordingly, (46) entails

$$\Phi_0(\mathbf{r}) = -z - \frac{a^3}{2}\sum_{m=0}^{\infty}\left\{\frac{z+\dfrac{a}{m+1}}{\left[r^2+\dfrac{a^2}{(m+1)^2}+\dfrac{2az}{m+1}\right]^{3/2}} + \frac{z-\dfrac{a}{m+1}}{\left[r^2+\dfrac{a^2}{(m+1)^2}-\dfrac{2az}{m+1}\right]^{3/2}}\right\}\frac{(-1)^m}{(m+1)^3}. \tag{49}$$

It is worthwhile noting that as $m\to\infty$ terms of this series behave as $O(m^{-3})$, ensuring fast, absolute convergence.

B. First-order approximation

1. Formulas for nontouching spheres, d>a

With $\Phi\sim\Phi_0+\Phi_1$ everywhere the boundary condition for Φ_1 on each spherical surface reads

$$\left.\frac{\partial\Phi_1}{\partial r'}\right|_{r'=a} = \frac{1}{\xi}\,(\Phi_0 - \varphi_0)|_{r'=a}, \tag{50}$$

where (r', θ', ϕ') is the coordinate system with origin at the center of each sphere and φ_0 is given by (19). By expanding Φ_0 in spherical harmonics according to (D1) and (D2) of Appendix D, condition (50) reads

$$\left.\frac{\partial\Phi_1}{\partial r'}\right|_{r'=a} = \frac{1}{\xi}\left[-a\cos\theta' - \frac{a}{2}\sum_{l=1}^{\infty} D_l P_l(\cos\theta)\right], \tag{51}$$

where

$$D_l = D_l^A = (\sinh\kappa)^3 l \sum_{m=0}^{\infty} \frac{(-1)^m}{[\sinh(m+1)\kappa]^3}\left[\left(\frac{\chi_m}{a}\right)^{l-1} + \left(1+\frac{1}{l}\right)\left(\frac{2d-\chi_m}{a}\right)^{-l-2}\right] \tag{52}$$

for sphere A, and

$$D_l = D_l^B = (\sinh\kappa)^3(-1)^{l-1} l \sum_{m=0}^{\infty} \frac{(-1)^m}{[\sinh(m+1)\kappa]^3}\left[\left(\frac{\chi_m}{a}\right)^{l-1} - \left(1+\frac{1}{l}\right)\left(\frac{2d-\chi_m}{a}\right)^{-l-2}\right] \tag{53}$$

for sphere B.

Therefore, Φ_1 is expanded inside each sphere as

$$\Phi_1 = -\frac{a}{\xi} r' \cos\theta' - \frac{a^2}{2\xi}\sum_{l=1}^{\infty}\frac{D_l}{l}\left(\frac{r'}{a}\right)^l P_l(\cos\theta') + \mathcal{C}, \tag{54}$$

where $\mathcal{C}$ is an immaterial constant which is henceforth set to zero, $\mathcal{C}=0$. In view of (52) and (53) along with (D1)–(D3) of Appendix D, carrying out the summation over l gives

$$\Phi_1 = -\frac{a}{\xi} z' - \frac{a^2}{2\xi}\sum_{m=0}^{\infty}(-1)^m \frac{(\sinh\kappa)^3}{[\sinh(m+1)\kappa]^3}\left[\frac{r'}{a} T_m\left(\mp\beta_m\frac{r'}{a}, \theta'\right) \pm \gamma_m^3 \frac{r'}{a} T_m\left(\mp\gamma_m\frac{r'}{a}, \theta'\right) + \gamma_m^2 S_m\left(\mp\gamma_m\frac{r'}{a}, \theta'\right)\right], \tag{55}$$

where the upper (lower) sign corresponds to cell A (B),

$$\beta_m = \frac{\sinh(m\kappa)}{\sinh[(m+1)\kappa]}, \quad \gamma_m = \left(\frac{2d-\chi_m}{a}\right)^{-1}, \tag{56}$$

$$T_m(s,\theta') = \frac{2\cos\theta' + s}{\sqrt{1+2s\cos\theta'+s^2}}\,\frac{1}{1+\sqrt{1+2s\cos\theta'+s^2}}, \tag{57}$$

$$S_m(s,\theta') = \ln\left|\frac{2}{\sin^2\theta'}\frac{1}{s}\right| + \ln\left|\frac{s+\cos\theta' - \cos\theta'\sqrt{1+2s\cos\theta'+s^2}}{1+\sqrt{1+2s\cos\theta'+s^2}}\right|, \tag{58}$$

and χ_m is defined by (44).

The electric field, which is proportional to the current, inside each cell is

$$\mathbf{E}_1 = -\mathbf{e}_{r'}\frac{\partial\Phi_1}{\partial r'} - \mathbf{e}_{\theta'}\frac{1}{r'}\frac{\partial\Phi_1}{\partial\theta'}, \tag{59}$$

where

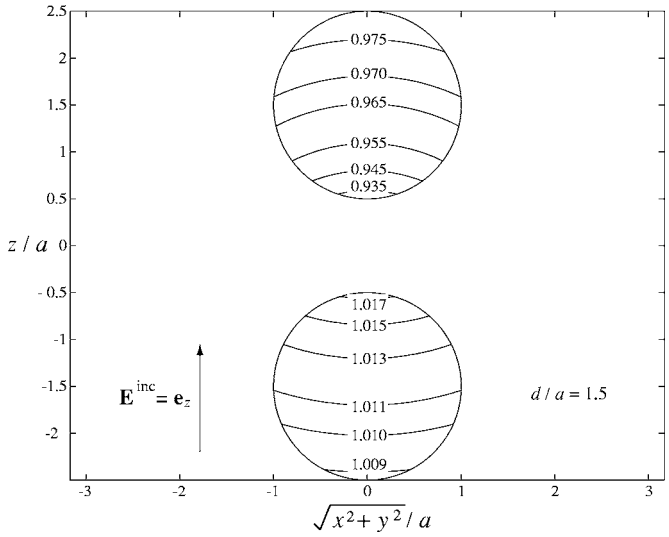

FIG. 3. Contour plots of the magnitude of the normalized electric field, $(3a/2\xi)^{-1}|\mathbf{E}_1|$, inside each cell. Maximum magnitudes are attained at $\theta'=0$; (x,y,z) is the usual Cartesian coordinate system.

$$-\frac{\partial\Phi_1}{\partial r'} = \frac{a}{\xi}\cos\theta' + \frac{a}{2\xi}\sum_{m=0}^{\infty}(-1)^m\frac{(\sinh\kappa)^3}{[\sinh(m+1)\kappa]^3} \times\left[V_m\left(\mp\beta_m\frac{r'}{a},\theta'\right)\pm\gamma_m^3 V_m\left(\mp\gamma_m\frac{r'}{a},\theta'\right)\pm\gamma_m^3 T_m\left(\mp\gamma_m\frac{r'}{a},\theta'\right)\right], \tag{60}$$

and

$$\frac{1}{r'}\frac{\partial\Phi_1}{\partial\theta'} = \frac{a}{\xi}\sin\theta' + \frac{a}{2\xi}\sin\theta'\sum_{m=0}^{\infty}(-1)^m\frac{(\sinh\kappa)^3}{[\sinh(m+1)\kappa]^3} \times\left[U_m\left(\mp\beta_m\frac{r'}{a},\theta'\right)\pm\gamma_m^3 U_m\left(\mp\gamma_m\frac{r'}{a},\theta'\right)\pm\gamma_m^3 W_m\left(\mp\gamma_m\frac{r'}{a},\theta'\right)\right]. \tag{61}$$

In the above,

$$U_m(s,\theta') = \frac{1}{(1+2s\cos\theta'+s^2)^{3/2}}, \tag{62}$$

$$V_m(s,\theta') = \frac{\cos\theta'+s}{(1+2s\cos\theta'+s^2)^{3/2}}, \tag{63}$$

$$W_m(s,\theta') = \frac{1}{\sqrt{1+2s\cos\theta'+s^2}}\,\frac{2\cos\theta'+s}{\cos\theta'(1+\sqrt{1+2s\cos\theta'+s^2})+s}. \tag{64}$$

In Fig. 3 we show contour plots for the magnitude of $\mathbf{E}_1$, normalized by the field $3a/2\xi$ inside an isolated spherical cell of equal radius (cf. Appendix A), inside cells A and B for a fixed value of d/a. In Fig. 4 we show plots for the maximum normalized magnitudes as functions of d/a. Two comments are in order: (i) As expected by close inspection of (59)–(64), for any $d>a$ the maximum $|\mathbf{E}_1|$ is attained for $\theta'=0$ for both spheres. (ii) This maximum value increases with d in sphere A and decreases with d in sphere B; cf. Fig. 4.

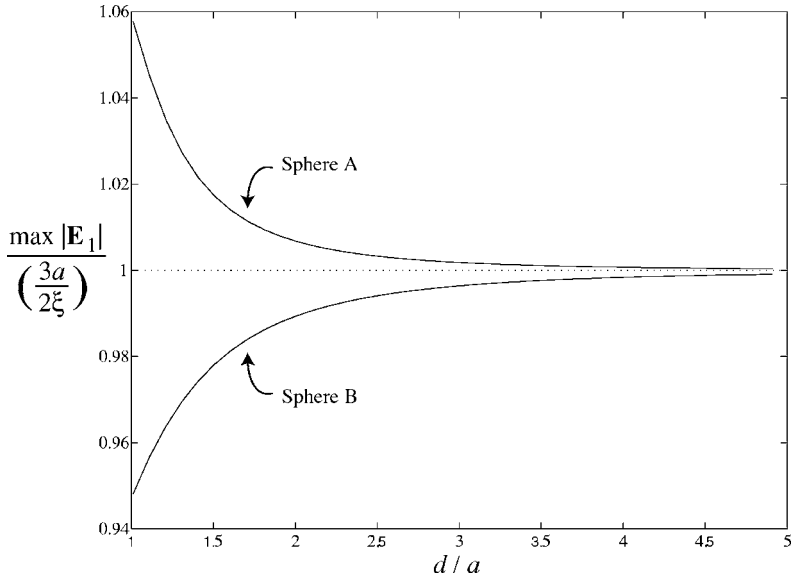

FIG. 4. Plots of the maximum magnitudes of the normalized electric fields inside cells A and B as functions of their normalized distance, d/a; $3a/2\xi$ is the electric field inside an isolated spherical cell of equal radius.

2. Touching spheres, $d\to a$

As mentioned above, a close examination of Eqs. (60) and (61) reveals that for fixed distance d the field magnitude attains its maximum at $\theta'=0$ inside sphere A (as r' approaches a from left, $r'\to a^-$). A similar situation arises in fluid mechanics.[21] This maximum increases as d approaches a when the spheres tend to touch. In this case, $d\to a$, approximation (47) yields

$$\Phi_1 = -\frac{a}{\xi}z' - \frac{a}{2\xi}\sum_{m=0}^{\infty}\frac{(-1)^m}{(m+1)^3}\left[\frac{r'}{a}T_m\left(\mp\frac{m}{m+1}\frac{r'}{a},\theta'\right) \pm \frac{(m+1)^3}{(m+2)^3}\frac{r'}{a}T_m\left(\mp\frac{m+1}{m+2}\frac{r'}{a},\theta'\right) + \frac{(m+1)^2}{(m+2)^2}S_m\left(\mp\frac{m+1}{m+2}\frac{r'}{a},\theta'\right)\right]. \tag{65}$$

The corresponding electric field is derived by invoking

$$-\frac{\partial\Phi_1}{\partial r'} = \frac{a}{\xi}\cos\theta' + \frac{a}{2\xi}\sum_{m=0}^{\infty}\frac{(-1)^m}{(m+1)^3}\left[V_m\left(\mp\frac{m}{m+1}\frac{r'}{a},\theta'\right) \pm \frac{(m+1)^3}{(m+2)^3}V_m\left(\mp\frac{m+1}{m+2}\frac{r'}{a},\theta'\right) \pm \frac{(m+1)^3}{(m+2)^3}T_m\left(\mp\frac{m+1}{m+2}\frac{r'}{a},\theta'\right)\right], \tag{66}$$

and

$$\frac{1}{r'}\frac{\partial\Phi_1}{\partial\theta'} = \frac{a}{\xi}\sin\theta' + \frac{a}{2\xi}\sin\theta'\sum_{m=0}^{\infty}\frac{(-1)^m}{(m+1)^3}\left[U_m\left(\mp\frac{m}{m+1}\frac{r'}{a},\theta'\right) \pm \frac{(m+1)^3}{(m+2)^3}U_m\left(\mp\frac{m+1}{m+2}\frac{r'}{a},\theta'\right) \pm \frac{(m+1)^3}{(m+2)^3}W_m\left(\mp\frac{m+1}{m+2}\frac{r'}{a},\theta'\right)\right]. \tag{67}$$

It follows that for $d\to a$ the electric field in sphere A along the z axis becomes $\mathbf{E}=(a/\xi)\mathcal{E}_1(z')\mathbf{e}_z$, where $\mathcal{E}_1$ is the positive quantity

$$\mathcal{E}_1(z') = 1 + \frac{1}{2}\sum_{m=0}^{\infty} \frac{(-1)^m}{(m+1)^3}\left(1 - \frac{|z'|}{a}\frac{m}{m+1}\right)^{-2} + \frac{1}{2}\sum_{m=0}^{\infty} \frac{(-1)^m}{(m+2)^3}\left(1 - \frac{|z'|}{a}\frac{m+1}{m+2}\right)^{-2}$$
$$+ \frac{1}{2}\sum_{m=0}^{\infty} \frac{(-1)^m}{(m+2)^3}\left(1 - \frac{|z'|}{a}\frac{m+1}{m+2}\right)^{-1}. \tag{68}$$

Hence, $\mathcal{E}_1$ attains its maximum for $z'=a$,

$$\mathcal{E}_{1,\max} = 1 + \frac{1}{2}\sum_{m=0}^{\infty} (-1)^m\left(\frac{1}{m+1} + \frac{1}{m+2} + \frac{1}{(m+2)^2}\right) = 2 - \frac{\pi^2}{24} \approx 1.5888, \tag{69}$$

which is 6% higher than the corresponding value inside the isolated spherical cell of equal radius; compare with (31) of Sec. II.

IV. CONCLUSION

By use of perturbation theory we studied analytically a mathematical model for the scattering of extremely low frequency, uniform electric fields from cells of arbitrary shapes. Two main assumptions in our derivations were that the cell radius of curvature is a slowly varying function of surface coordinates and the cell interior is an isotropic and homogeneous medium. Our results for two spherical cells suggest that the presence of a neighboring cell causes only a small increase to the electric field inside a single cell of reasonably arbitrary shape.

Our analysis, based on suitable application of regular perturbations along with a reflection principle and exact solution of a nonlinear difference equation, can be extended to geometries of many cells but becomes increasingly cumbersome with the number of cells. In this case the solution for the electrostatic potential is obtained by solving a system of tractable difference equations. It is expected, however, that the presence of additional cells will cause only a minor increase in the induced electric field, being sufficiently bounded in the number of cells. This problem is subject of work in progress.

ACKNOWLEDGMENTS

The authors are indebted to Professor T. T. Wu for suggesting the problem.

APPENDIX A: REVISITING THE SINGLE SPHERICAL CELL

In this appendix we review the case with a uniform electric field incident on a single spherical cell, which is also studied in Refs. 2 and 4. The cell interior consists of two concentric spheres of radii a and b, where $b>a$. The effective dielectric constant in the regions $0<r<a$ and $r>b$ is taken to be 1 without loss of generality; the region $a<r<b$ corresponds to the cell membrane and has dielectric constant equal to the ϵ defined by (2). The real parameter ϵ expresses the *relative* dielectric constant for the two media, membrane and protoplasm, and is equal to the ratio of their conductivities, which enter the equations only through the homogeneous boundary conditions given in Eqs. (A5) and (A6) below. For an incident field $\mathbf{E}^{\text{inc}}=\mathbf{e}_z$ the scalar potential Φ at infinity is

$$\Phi(r,\theta) \sim -r\cos\theta, \quad r\to\infty, \tag{A1}$$

where (r,θ,ϕ) are the usual spherical coordinates. The boundary conditions at $r=a,b$ dictate continuity of Φ and $\epsilon(\partial\Phi/\partial r)$ across the spherical boundaries. The scalar potential Φ is thus independent of the azimuthal angle, ϕ, while it satisfies Laplace's equation in free space. With

$$\Phi(r,\theta) = f(r)\cos\theta, \tag{A2}$$

we obtain the equation

$$\left(\frac{d^2}{dr^2}+\frac{2}{r}\frac{d}{dr}-\frac{2}{r^2}\right)f(r)=0, \tag{A3}$$

with general solution $f(r)=Ar+Br^{-2}$. More precisely,

$$f(r)=\begin{cases} A_1 r, & r<a, \\ A_2 r+\dfrac{B_2}{r^2}, & a<r<b, \\ -r+\dfrac{B_3}{r^2}, & r>b, \end{cases} \tag{A4}$$

where the boundary condition (A1) has been used. In order to determine the constants A_1, A_2, B_2, and B_3 we apply the boundary conditions at $r=a$ and $r=b$, and thus obtain the equations

$$A_1 a=A_2 a+\frac{B_2}{a^2}, \quad A_1=\epsilon\left(A_2-\frac{2B_2}{a^3}\right), \tag{A5}$$

$$A_2 b+\frac{B_2}{b^2}=-b+\frac{B_3}{b^2}, \quad \epsilon\left(A_2-\frac{2B_2}{b^3}\right)=-1-\frac{2B_3}{b^3}. \tag{A6}$$

The electric field inside the cell is $-A_1\mathbf{e}_z$, where

$$-A_1=\frac{9\epsilon}{(1+2\epsilon)(2+\epsilon)-2(1-\epsilon)^2(a/b)^3}. \tag{A7}$$

Specifically, if ϵ is small and $a=b-\delta$, $\delta\ll a$, then

$$-A_1\sim\frac{1}{1+\dfrac{2}{3}\dfrac{\delta}{a\epsilon}}=\frac{1}{1+\dfrac{2\xi}{3a}}, \tag{A8}$$

where $\xi=\delta/\epsilon$. The right-hand side of the above equation is small if $\xi\gg a$, and can be expanded as a (convergent) geometric series for $3a/(2\xi)<1$. Specifically,

$$-A_1\sim\frac{3a}{2\xi}, \quad \frac{a}{\xi}\ll 1. \tag{A9}$$

APPENDIX B: REFLECTION PRINCIPLE WITH NEUMANN CONDITION

In this appendix (i) we derive a reflection principle, involving image dipoles, for the problem with a source dipole in the presence of a sphere with Neumann boundary conditions, extending the known analysis with a source charge and Dirichlet boundary conditions;[20] and (ii) we apply this principle to determine the potential Φ for the case with an insulating sphere and incident uniform electric field (cf. Appendix A).

We consider a $\mathbf{z}$-directed electric dipole of moment $\mathbf{p}=p\mathbf{e}_z$ located at $\mathbf{r}_0=(0,0,h)$ in the presence of a sphere with radius a centered at O. In units where $\epsilon_{\text{eff}}=1$, where ϵ_{eff} is the effective dielectric constant of the infinite medium, the ensuing scalar potential $\Phi(\mathbf{r};\mathbf{r}_0|\mathbf{p})$ satisfies the Poisson equation

$$\nabla^2\Phi=p\frac{\partial}{\partial z}\delta(\mathbf{r}-\mathbf{r}_0), \quad r>a, \tag{B1}$$

along with the prescribed Neumann boundary condition

$$\left.\frac{\partial\Phi}{\partial r}\right|_{r=a}=0, \tag{B2}$$

and $\Phi(\mathbf{r};\mathbf{r}_0|\mathbf{p})\to 0$ as $r\to\infty$. The potential Φ is thus determined uniquely in the region $r>a$. Recall that the potential generated by a dipole of moment $\mathbf{p}$ located at the origin is $\mathbf{p}\cdot\mathbf{r}/4\pi r^3$. We next express Φ for $r>a$ as a superposition of the (primary) potential Φ^{pr} generated by the source dipole at $\mathbf{r}_0$ in the absence of the sphere and the (scattered) potential Φ^{sc} of an image dipole with moment $\mathbf{p}'=\nu p\mathbf{e}_z$ at $\mathbf{r}_1=(0,0,h')$ where $h'<a$; ν and h' are to be determined.

Because of condition (B2) it is advantageous to work directly with the electric field $\mathbf{E}=-\nabla\Phi$. For $r>a$ and $|\mathbf{r}-\mathbf{r}_0|>0$,

$$\begin{aligned}\mathbf{E}(\mathbf{r})=\mathbf{E}^{\mathrm{pr}}(\mathbf{r})+\mathbf{E}^{\mathrm{sc}}(\mathbf{r})&=\frac{3[\mathbf{p}\cdot(\mathbf{r}-\mathbf{r}_0)](\mathbf{r}-\mathbf{r}_0)-(\mathbf{r}-\mathbf{r}_0)^2\mathbf{p}}{4\pi|\mathbf{r}-\mathbf{r}_0|^5}+\nu\frac{3[\mathbf{p}'\cdot(\mathbf{r}-\mathbf{r}_1)](\mathbf{r}-\mathbf{r}_1)-(\mathbf{r}-\mathbf{r}_1)^2\mathbf{p}'}{4\pi|\mathbf{r}-\mathbf{r}_1|^5}\\&=p\frac{3(r\cos\theta-h)(r\mathbf{e}_r-h\mathbf{e}_z)-(r^2+h^2-2rh\cos\theta)\mathbf{e}_z}{4\pi(r^2+h^2-2rh\cos\theta)^{5/2}}\\&\quad+\nu p\frac{3(r\cos\theta-h')(r\mathbf{e}_r-h'\mathbf{e}_z)-(r^2+h'^2-2rh'\cos\theta)\mathbf{e}_z}{4\pi(r^2+h'^2-2rh'\cos\theta)^{5/2}}.\end{aligned} \tag{B3}$$

Hence,

$$-\left.\frac{\partial\Phi(\mathbf{r})}{\partial r}\right|_{r=a}=p\frac{2(a^2+h^2)\cos\theta-ah(3+\cos^2\theta)}{4\pi(a^2+h^2-2ah\cos\theta)^{5/2}}+\nu p\frac{2(a^2+h'^2)\cos\theta-ah'(3+\cos^2\theta)}{4\pi(a^2+h'^2-2ah'\cos\theta)^{5/2}}. \tag{B4}$$

The substitution

$$\frac{h'}{a}=\frac{a}{h} \tag{B5}$$

yields $|\mathbf{r}-\mathbf{r}_1|=(a/h)|\mathbf{r}-\mathbf{r}_0|$ and reduces (B4) to

$$-\left.\frac{\partial\Phi(\mathbf{r})}{\partial r}\right|_{r=a}=p\left[1+\nu\left(\frac{h}{a}\right)^3\right]\frac{2(a^2+h^2)\cos\theta-ah(3+\cos^2\theta)}{4\pi(a^2+h^2-2ah\cos\theta)^{5/2}}. \tag{B6}$$

Condition (B2) is satisfied if

$$\nu=-\frac{a^3}{h^3}. \tag{B7}$$

This equation concludes the derivation of the reflection principle for a source dipole and Neumann boundary condition on a neighboring sphere.

Next, we apply this principle in order to derive the electrostatic potential for the case with an insulating sphere immersed in a uniform electric field, $E^{\mathrm{inc}}=E_0\mathbf{e}_z$; cf. Appendix A. This potential satisfies the Laplace equation and condition (B2), while the condition at infinity reads

$$\Phi(\mathbf{r})\sim -E_0 r\cos\theta \quad \text{as } r\to\infty. \tag{B8}$$

The uniform incident field is now viewed as the total field of two dipoles located at $(0,0,h)$ and $(0,0,-h)$ in the limit $h\to\infty$, where each dipole has moment $\mathbf{p}=p\mathbf{e}_z$.[22] The scalar potential due to these dipoles in the presence of the insulating sphere and for $r>a$ is

$$\Phi(\mathbf{r}) = \frac{p}{4\pi h^3}\left[\frac{r\cos\theta - h}{\left(1 - \frac{2r}{h}\cos\theta + \frac{r^2}{h^2}\right)^{3/2}} - \frac{a^3}{r^3}\frac{r\cos\theta - \frac{a^2}{h}}{\left(1 - \frac{2a^2}{hr}\cos\theta + \frac{a^4}{r^2h^2}\right)^{3/2}} + \frac{r\cos\theta + h}{\left(1 + \frac{2r}{h}\cos\theta + \frac{r^2}{h^2}\right)^{3/2}}\right.$$
$$\left. - \frac{a^3}{r^3}\frac{r\cos\theta + \frac{a^2}{h}}{\left(1 + \frac{2a^2}{hr}\cos\theta + \frac{a^4}{r^2h^2}\right)^{3/2}}\right] = -\frac{p}{\pi h^3}\left[r + \frac{a^3}{2r^2} + O\left(\frac{a^5}{r^5}\frac{a^2}{h^2}\right)\right]\cos\theta$$
$$\equiv -E_0\left(r + \frac{a^3}{2r^2}\right)\cos\theta, \quad h \to \infty, \tag{B9}$$

in view of (B8), where

$$p = \pi h^3 E_0, \quad h \to \infty. \tag{B10}$$

APPENDIX C: SOLUTION OF NONLINEAR DIFFERENCE EQUATION

In this appendix, the difference equation

$$x_n = \frac{\tilde{a}^2}{1 - x_{n-1}}, \quad n = 1,2,\ldots, \tag{C1}$$

where $0 < \tilde{a} \leqslant 1/2$ and $x_0 < 0$, is solved exactly. The solution is subsequently simplified for $|x_0| \ll 1$.

The substitution $x_n = \tilde{a}(y_n/y_{n+1})$ recasts (C1) to

$$y_n = \tilde{a}(y_{n+1} + y_{n-1}), \quad n = 1,2,\ldots. \tag{C2}$$

This equation is linear and can be solved via the replacement $y_n = \varrho^n$. The variable ϱ satisfies the equation $\tilde{a}\varrho^2 - \varrho + \tilde{a} = 0$ with solutions

$$\varrho = \varrho_\pm = \frac{1 \pm \sqrt{1 - 4\tilde{a}^2}}{2\tilde{a}}. \tag{C3}$$

Note that $\varrho_+\varrho_- = 1$ and $\varrho_+ + \varrho_- = 1/\tilde{a}$. It is inferred that $\varrho_+ \geqslant 1$ and $0 < \varrho_- \leqslant 1$. The solution to (C2) thus reads

$$y_n = c_1\varrho_+^n + c_2\varrho_-^n, \tag{C4}$$

where c_1 and c_2 are constants. Accordingly,

$$x_n = \tilde{a}\lambda\frac{\tilde{c}\lambda^{2n} - 1}{\tilde{c}\lambda^{2(n+1)} - 1}, \quad \lambda = \varrho_+, \quad \tilde{c} = -\frac{c_1}{c_2}. \tag{C5}$$

It follows that

$$\tilde{c} = \frac{\tilde{a} + \lambda^{-1}|x_0|}{\tilde{a} + \lambda|x_0|}, \quad 0 < \tilde{c} < 1. \tag{C6}$$

Let

$$\tilde{c} = e^{-2\zeta}, \quad \lambda = e^{\kappa}, \quad \zeta > 0, \quad \kappa > 0. \tag{C7}$$

Equation (C5) then becomes

$$x_n = \tilde{a}\frac{\sinh(n\kappa - \zeta)}{\sinh[(n+1)\kappa - \zeta]}, \quad n = 0,1,2,\ldots . \tag{C8}$$

It remains to derive an approximation for x_n when $\tilde{a}^{-1}|x_0| \ll 1$. From (C6),

$$\tilde{c} \sim (1 - \tilde{a}^{-1}\lambda^{-1}x_0)(1 + \tilde{a}^{-1}\lambda x_0) \sim 1 + (1 - \lambda^{-2})\tilde{a}^{-1}\lambda x_0, \tag{C9}$$

which in turn leads to

$$x_n \sim \tilde{a}\frac{[1 - (1 - e^{-2\kappa})\tilde{a}^{-1}\lambda|x_0|]e^{n\kappa} - e^{-n\kappa}}{[1 - (1 - e^{-2\kappa})\tilde{a}^{-1}\lambda|x_0|]e^{(n+1)\kappa} - e^{-(n+1)\kappa}} \sim \tilde{a}\frac{\sinh n\kappa}{\sinh(n+1)\kappa}\left(1 - e^{n\kappa}\frac{\sinh\kappa}{\sinh n\kappa}\tilde{a}^{-1}|x_0|\right)$$
$$\times\left[1 + \tilde{a}^{-1}|x_0|e^{(n+1)\kappa}\frac{\sinh\kappa}{\sinh(n+1)\kappa}\right] \sim \tilde{a}\frac{\sinh n\kappa}{\sinh(n+1)\kappa} - \left[\frac{\sinh\kappa}{\sinh(n+1)\kappa}\right]^2|x_0|. \tag{C10}$$

This expression becomes a trivial equality for $n=0$. Note that the coefficient of the correction term $O(x_0)$ is bounded uniformly with n.

APPENDIX D: ELEMENTARY EXPANSION IN LEGENDRE POLYNOMIALS

It is known that[23]

$$(1 + 2\beta x + \beta^2)^{-1/2} = \sum_{l=0}^{\infty}(-1)^l \mathrm{P}_l(x)\begin{cases}\beta^l, & |\beta| < 1,\\ \beta^{-l-1}, & |\beta| > 1,\end{cases} \tag{D1}$$

where $x = \cos\theta$ and $\mathrm{P}_l(x)$ are Legendre polynomials. It follows by differentiation that

$$\frac{x+\beta}{(1 + 2\beta x + \beta^2)^{3/2}} = \sum_{l=0}^{\infty}(-1)^l \mathrm{P}_l(x)\begin{cases}(-l)\beta^{l-1},\\ (l+1)\beta^{-l-2},\end{cases} \tag{D2}$$

for $|\beta| < 1$ or $|\beta| > 1$, respectively.

The term-by-term integration of (D1) yields

$$\sum_{l=1}^{\infty}\frac{\beta^l}{l}\mathrm{P}_l(x) = \int_0^{\beta}\frac{\mathrm{d}t}{t}\left(\frac{1}{\sqrt{1 - 2tx + t^2}} - 1\right), \tag{D3}$$

where $|\beta| < 1$. This integral is elementary; by changing the variable to w according to $t - x = \sqrt{1 - x^2}\sinh w$ we find

$$\sum_{l=1}^{\infty}\frac{\beta^l}{l}\mathrm{P}_l(x) = \ln\left|\frac{2}{1-x^2}\frac{1}{\beta}\frac{\beta - x + x\sqrt{1 - 2\beta x + \beta^2}}{1 + \sqrt{1 - 2\beta x + \beta^2}}\right|. \tag{D4}$$

In the limit $x \to 1^-$ the right-hand side of this formula approaches $-\ln(1-\beta)$, as it should.

[1] *Biological Effects and Medical Applications of Electromagnetic Energy*, edited by O. P. Gandhi (Prentice-Hall, Englewood Cliffs, NJ, 1990).
[2] R. K. Adair, Phys. Rev. A **43**, 1039 (1991).
[3] R. W. P. King and T. T. Wu, J. Appl. Phys. **78**, 668 (1995).
[4] R. W. P. King and T. T. Wu, Phys. Rev. E **58**, 2363 (1998).
[5] E. C. Fear and M. A. Stuchly, IEEE Trans. Biomed. Eng. **45**, 856 (1998).
[6] R. W. P. King, Radio Sci. **34**, 539 (1999).
[7] R. K. Aaron, D. M. Ciombor, H. Keeping, S. Wang, A. Capuano, and C. Polk, Bioelectromagnetics (N.Y.) **20**, 453 (1999); **21**, 73(E) (2000).
[8] R. W. P. King and T. T. Wu, Radiat. Res. **153**, 715 (2000).
[9] J. H. Lee and K. J. McLeod, Bioelectromagnetics (N.Y.) **21**, 129 (2000).
[10] R. W. P. King, Radio Sci. **36**, 1653 (2001).
[11] R. W. P. King and D. Margetis, in *Progress in Electromagnetic Research*, edited by J. A. Kong (EMW Publishing, Cambridge, MA, 2002), Vol. 36, p. 61; J. Electromagn. Waves Appl. **16**, 907 (2002).

[12] B. Alberts, D. Bray, J. Lewis, M. Raff, K. Roberts, and J. D. Watson, *Molecular Biology of the Cell* (Garland, New York, 1994), Chap. 11.
[13] J. Kevorkian and J. D. Cole, *Perturbation Methods in Applied Mathematics* (Springer-Verlag, New York, 1981).
[14] The term "interior" in the case with a membrane of finite thickness defines the region occupied by the cell with the exclusion of the membrane. In the limit of vanishingly small membrane thickness the interior does not include the boundary; the rest of space, including the boundary, is the "exterior" of the cell.
[15] As mentioned in the Introduction, elongated cells may be excluded from our analysis.
[16] The issue of convergence of this expansion is not addressed in this paper. It is expected that the expansion converges for sufficiently small r_c/ξ.
[17] The perturbation order n (subscript in expansion terms) should not be confused with the index j in $\mathcal{R}_j$, $\partial\mathcal{R}_j$ and other symbols of this section; j specifies individual cells.
[18] $A=O(x_1,x_2,\ldots,x_N)$ as $\mathbf{x}=(x_1,x_2,\ldots,x_N)\to 0$ means that $\lim_{\mathbf{x}\to 0}(A/x_k)=O(1)$ if $x_j/x_k=O(1)$ for all $j,k=1,2,\ldots,N$.
[19] E. DiBenedetto, *Partial Differential Equations* (Birkhäuser, Boston, 1995), Chap. II.
[20] J. D. Jackson, *Classical Electrodynamics* (Wiley, New York, 1999), Chap. 2.
[21] J. C. Baygents, N. J. Rivette, and H. A. Stone, J. Fluid Mech. **368**, 359 (1998).
[22] The reason for considering two symmetrically located dipoles instead of one is the ensuing convenience of eliminating any residual constant for the potential Φ in the limit $h\to\infty$. Specifically, Φ remains zero at the origin for any distance h $(h>0)$.
[23] Bateman Manuscript Project, *Higher Transcendental Functions*, edited by A. Erdélyi (McGraw-Hill, New York, 1953), Vol. I, p. 154.